Electronic Supplementary Information

Rationally designed organelle-specific thermally activated delayed fluorescence small molecular organic probes for time-resolved biological applications

Qingyang Zhang,[†a] Shengnan Xu,[†a] Meng Li,[†b] Yali Wang,[a] Na Zhang,[a] Yan Guan,[c] Mingxing Chen,[c] Chuan-Feng Chen[*b] and Hai-Yu Hu[*a]

[a]*State Key Laboratory of Bioactive Substances and Function of Natural Medicine, Beijing Key Laboratory of Active Substances Discovery and Drugability Evaluation, Institute of Materia Medica, Chinese Academy of Medical Sciences & Peking Union Medical College, Beijing, 100050, China*

[b]*CAS Key Laboratory of Molecular Recognition and Function, Institute of Chemistry, Chinese Academy of Sciences, Beijing, 100190, China*

[c]*Analytical Instrumentation Center, College of Chemistry and Molecular Engineering, Peking University, Beijing, 100871, China*

[†]Q. Zhang, S. Xu and M. Li contributed equally to this work.

Email: haiyu.hu@imm.ac.cn; cchen@iccas.ac.cn

Contents

1. Abbreviations

ATCC = American Type Culture Collection

BSA = Bovine Serum Albumin

DCM = Dichloromethane

Diox = 1,4-Dioxane

DIPEA = *N*,*N*-Diisopropylethylamine

DMF = Dimethylformamide

DMSO = Dimethyl Sulfoxide

EA = Ethyl Acetate

FBS = Fetal Bovine Serum

FLIM = Fluorescence Lifetime Imaging Microscopy

HATU = 2-(7-Azabenzotriazol-1-yl)-*N*,*N*,*N'*,*N'*-tetramethyluronium Hexafluorophosphate

HRMS = High Resolution Mass Spectrometry

IRF = Instrument Response Function

LTR = Lyso Tracker Red DND-99

2-MeTHF = 2-Methyltetrahydrofuran

MTG = Mito Tracker Green

MTS = 3-(4,5-dimethylthiazol-2-yl)-5-(3-carboxymethoxyphenyl)-2-(4-sulfophenyl)-2H-tetrazolium

NMR = Nuclear Magnetic Resonance

PBS = Phosphate Buffer Saline

PE = Petroleum Ether

rt = Room Temperature

TADF = Thermally Activated Delayed Fluorescence

TFA = Trifluoroacetic Acid

THF = Tetrahydrofuran

2. General Methods

Commercially available reagents were used without further purification. Dulbecco's modified Eagle's medium (DMEM), fetal bovine serum (FBS) and penicillin− streptomycin solution (100×) were purchased from Corning. Bovine serum albumin (BSA) was purchased from Sigma-Aldrich. 3-(4,5-Dimethylthiazol-2-yl)-5-(3-carboxymethoxy-phenyl)-2-(4-sulfophenyl)-2H-tetrazolium (MTS) was purchased from Promega. Lyso Tracker Red DND-99 (LTR) and Mito Tracker Green (MTG) were purchased from Invitrogen (USA). Fluorescence emission spectra and full wavelength absorption spectra were performed on Tecan Spark™ 10M Multimode Microplate Reader. Fluorescence emission decays and fluorescence lifetimes of **AI-Cz-MT** and **AI-Cz-LT** under diffident conditions were measured with Edinburgh photonics FLS980 (laser model: VPL-375, the pulse width 500 ns). Confocal laser scanning microscope imaging were conducted with Leica TCS SP8 X Confocal Microscope. Fluorescence lifetime imaging were taken by ISS Q2 confocal laser scanning system coupled to a Nikon TE2000 microscope with the 60×/1.2 NA WI objective lens. All ^{1}H NMR spectra were recorded at 400 MHz, respectively. ^{13}C NMR spectra were recorded at 150 MHz, respectively. HRMS was measured with Thermo LCQ Deca XP Max mass spectrometer for ESI.

3. Uptake of lipophilic cations through phospholipid bilayers of mitochondrial

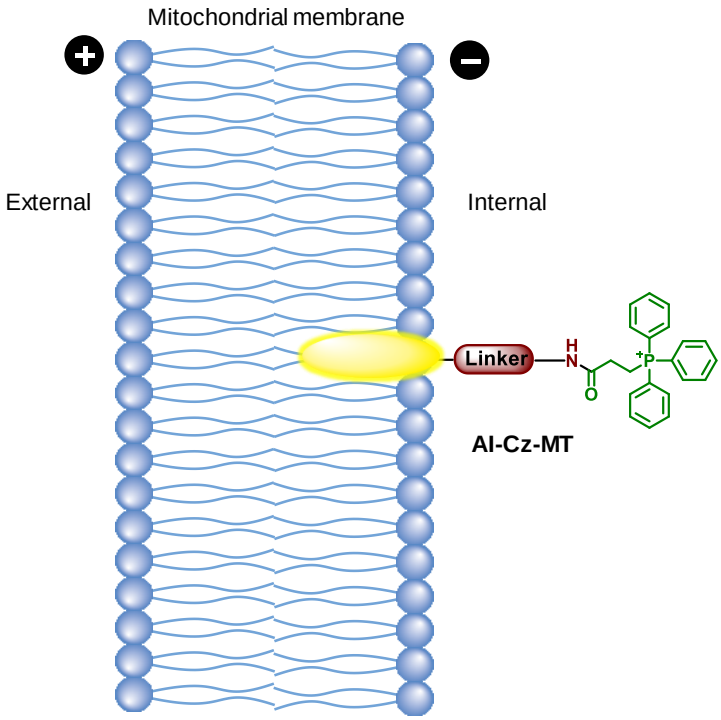

Fig. S1 Uptake of lipophilic cations through phospholipid bilayers of mitochondrial. **AI-Cz-MT** will be largely present adsorbed to the inner surface of the inner membrane, with the TPP moiety on the inner membrane surface and the lipophilic **AI-Cz** moiety inserted into the membrane.

4. Synthetic procedures and characterized data

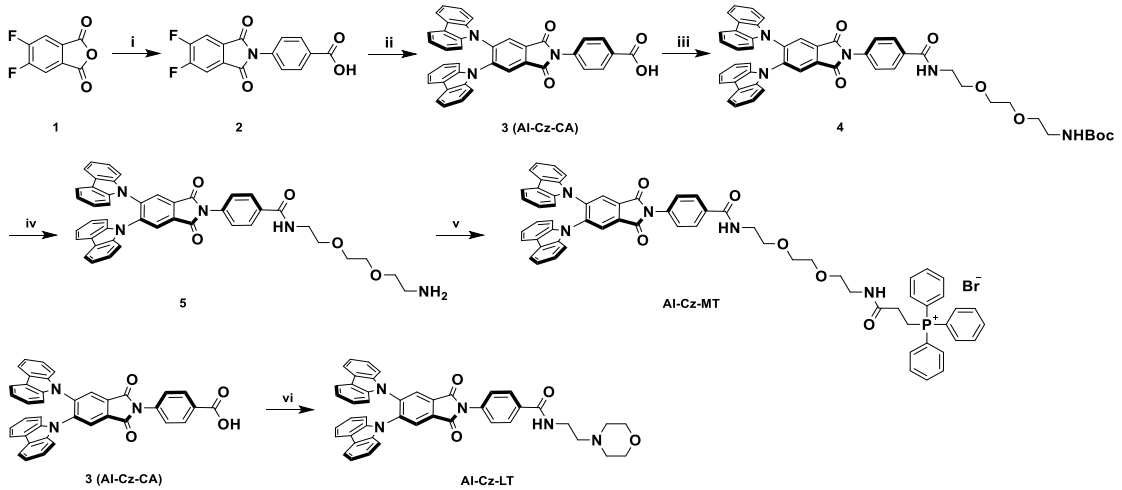

Scheme S1. Synthesis of **AI-Cz-MT** and **AI-Cz-LT**. Reagents and conditions: (i) 4-aminobenzoic acid, acetic acid, reflux, 4 h; (ii) NaH, carbazole, DMF, 0 °C, 2 h; (iii) tert-butyl(2-(2-(2-aminoethoxy)ethoxy)ethyl)carbamate, HATU, DIPEA, DMF, rt, 1 h; (iv) TFA, rt, 30 min; (v) (2-carboxyethyl)triphenylphosphonium bromide, HATU, DIPEA, DMF, rt, 1 h; (vi) 2-morpholinoethan-1-amine, HATU, DIPEA, DMF, rt, 1 h.

Compound **2**: Compound **1** (1 g, 5.43 mmol) and 4-aminobenzoic acid (1.12 g, 8.17 mmol) were added to acetic acid (30 mL) and the mixture was stirred and refluxed for 4 h. The solution was cooled down to 4 °C overnight, extraction filtration to give white solid 1.32 g, yield 80.0 %. mp > 230 °C; ^{1}H NMR (400 MHz, DMSO-d_6, δ): 13.14 (s, 1H, COOH), 8.22 (t, J = 7.6 Hz, 2H, Ar H), 8.11–8.08 (m, 2H, Ar H), 7.61–7.59 (m, 2H, Ar H). ^{13}C NMR (100 MHz, DMSO-d_6, δ): 167.1, 165.3, 155.0, 154.9, 153.3, 153.2, 136.0, 130.6, 130.3, 129.4, 127.4, 114.4, 114.3, 114.2, 114.2. HRMS (ESI) m/z: $[M + H]^+$ calcd for $C_{15}H_8O_4NF_2$, 304.0416; found 304.0411.

Compound **3** (**AI-Cz-CA**): Compound **2** (1 g, 3.30 mmol) was stirred in DMF (10 mL) at 0 °C and NaH (330 mg, 8.25 mmol) stage addition in an hour, then mixture with carbazole (1.65 g, 9.90 mmol) for 1 h. Extracted with EA (2 × 50 mL) and dried over Na_2SO_4. The residue was purified by silica gel column chromatography (PE : EA = 3 : 1) to give yellow solid 1.47 g, yield 75.6 %. mp > 230 °C; ^{1}H NMR (400 MHz, $CDCl_3$, δ): 8.48 (s, 2H, Ar H), 8.33 (d, J = 8.0 Hz 2H, Ar H), 7.80–7.78 (m, 4H, Ar H), 7.74 (d, J = 8.0 Hz 2H, Ar H), 7.16–7.14 (m, 4H, Ar H), 7.11–7.05 (m, 8H, Ar H). ^{13}C NMR (100 MHz, $CDCl_3$, δ): 170.9, 165.4, 139.7, 138.7, 136.5, 131.3, 130.6, 128.7, 126.1, 126.0, 125.9, 124.0, 121.1, 120.2, 109.3. HRMS (ESI) m/z: $[M + H]^+$ calcd for $C_{39}H_{24}O_4N_3$, 598.1761; found 598.1755.

Compound **4**: Compound **3** (200 mg, 0.33 mmol), HATU (153 mg, 0.40 mmol), DIPEA (87 mg, 0.67 mmol) was stirred in DMF (6 mL) at rt for 30 min. Then added tert-butyl(2-(2-(2-aminoethoxy)ethoxy)ethyl)carbamate (100 mg, 0.40 mmol) for 30 min. Extracted with EA (2 × 50 mL) and dried over Na_2SO_4. The residue was purified by silica gel column chromatography (PE : EA = 1 : 2) to give yellow solid 223 mg, yield 80.5 %. ^{1}H NMR (400 MHz, $CDCl_3$, δ): 8.47 (s, 1H, Ar H), 8.31 (s, 1H, Ar H), 8.01–7.96 (m, 2H, Ar H), 7.81–7.78 (m, 2H, Ar H), 7.71–7.69 (m, 2H, Ar H), 7.53–7.52 (m, 2H, Ar H), 7.16–7.10 (m, 4H, Ar H), 7.08–7.06 (m, 4H, Ar H), 7.01–6.98 (m, 4H, Ar H), 3.71–3.57 (m, 12H, CH_2), 1.44 (s, 6H, CH_3), 1.26 (s, 3H, CH_3). ^{13}C NMR (150 MHz, $CDCl_3$, δ): 165.5, 139.6, 139.5, 138.8, 138.7, 134.4, 134.1, 133.5, 130.7, 130.6, 128.2, 128.0, 126.2, 126.1, 126.0, 125.9, 125.8, 124.0, 123.9, 121.1, 121.0, 120.2, 120.1, 109.3, 109.3, 70.2, 70.0, 69.8, 66.5, 40.3, 39.9, 39.7, 29.7, 28.4. HRMS (ESI) m/z: $[M + H]^+$ calcd for $C_{50}H_{46}O_7N_5$, 828.3392; found 828.3384.

AI-Cz-MT: A mixture of compound **4** (100 mg, 0.12 mmol) in TFA (1 mL) at rt for 30 min and then TFA was evaporated to dryness to give crude compound **5**. Subsequently, (2-carboxyethyl)triphenylphosphonium bromide (50 mg, 0.12 mmol), HATU (55mg, 0.15 mmol), DIPEA (31mg, 0.24 mmol) was stirred in DMF (3 mL) at rt for 30 min and then mixture with unpurified compound **5** for 30 min. Extracted with EA (2 × 50 mL) and dried over Na_2SO_4. The residue was purified by silica gel column chromatography (PE : EA = 1 : 2) to give yellow solid 31 mg, yield 22.8 %. mp 109-110 °C; ^{1}H NMR (400 MHz, methanol-d_4, δ): 8.33 (d, J = 5.6 Hz, 2H, Ar H), 7.98 (d, J = 8.4 Hz, 2H, Ar H), 7.82–7.73 (m, 15H, Ar H), 7.69–7.68 (m, 4H, Ar H), 7.67–7.66 (m, 2H, Ar H), 7.20–7.17 (m, 4H, Ar H), 7.06–7.02 (m, 8H, Ar H), 3.70–3.64 (m, 6H, CH_2), 3.61–3.57 (m, 4H, CH_2), 3.48 (t, J = 5.2 Hz, 2H, CH_2), 3.25 (t, J = 5.2 Hz, 2H, CH_2), 2.66–2.59 (m, 2H, CH_2). ^{13}C NMR (100 MHz, methanol-d_4, δ): 171.3, 171.2, 169.3, 167.1, 140.7, 140.3, 136.4, 136.3, 135.1, 134.9, 134.8, 132.7, 131.6, 131.5, 129.1, 127.7, 127.5, 126.9, 126.8, 125.3, 122.0, 121.9, 121.1, 121.0, 119.9, 119.3, 110.7, 71.4, 70.5, 70.4, 41.0, 40.7, 28.9, 19.1, 18.8. HRMS (ESI) m/z: $[M]^+$ calcd for $C_{66}H_{55}O_6N_5P^+$, 1044.3884; found 1044.3885.

AI-Cz-LT: Compound **3** (200 mg, 0.33 mmol), HATU (153 mg, 0.40 mmol), DIPEA (87 mg, 0.67 mmol) was stirred in DMF (10 mL) at rt for 30 min. Then added 2-morpholinoethan-1-amine (52 mg, 0.40 mmol) for 30 min. Extracted with EA (2 × 50 mL), and dried over Na_2SO_4. The residue was purified by silica gel column chromatography (DCM : MeOH = 60 : 1) to give yellow solid 184 mg, yield 77.5 %. mp 135-136 °C; ^{1}H NMR (400 MHz, methanol-d_4, δ): 8.43 (s, 2H, Ar H), 8.08 (d, J = 8.4 Hz, 2H, Ar H), 7.83–7.79 (m, 4H, Ar H), 7.76 (d, J = 8.4 Hz, 2H, Ar H), 7.22–7.20 (m, 4H, Ar H), 7.09–7.00 (m, 8H, Ar H), 4.13–4.08 (m, 2H, CH_2), 3.83 (t, J = 5.6 Hz, 4H, CH_2), 3.73–3.69 (m, 2H, CH_2), 3.45 (t, J = 6 Hz, 2H, CH_2), 3.26–3.22 (m, 2H, CH_2). ^{13}C NMR (100 MHz, methanol-d_4, δ): 170.6, 167.1, 140.7, 140.4, 136.9, 133.9, 132.8, 129.3, 127.8, 126.9, 126.8, 125.3, 122.0, 121.1, 110.7, 65.2, 58.7, 53.7, 35.8. HRMS (ESI) m/z: $[M+H]^+$ calcd for $C_{45}H_{36}O_4N_5$, 710.2762; found 710.2741.

5. UV-Vis absorption and fluorescence spectra of AI-Cz, AI-Cz-MT and AI-Cz-LT

The stock solutions of the probes were prepared at 5 mM in DMSO. The concentration of DMSO stock solution of the probes was diluted to 10 μM in PBS (20 mM, pH 7.4) solution with 2% DMSO as the cosolvent with or without the addition of 10 mg/mL BSA. The UV-Visible spectra and fluorescence spectroscopic studies were recorded using a Tecan Spark™ 10M Multimode Microplate Reader. Wavelength interval: 5.0 nm.

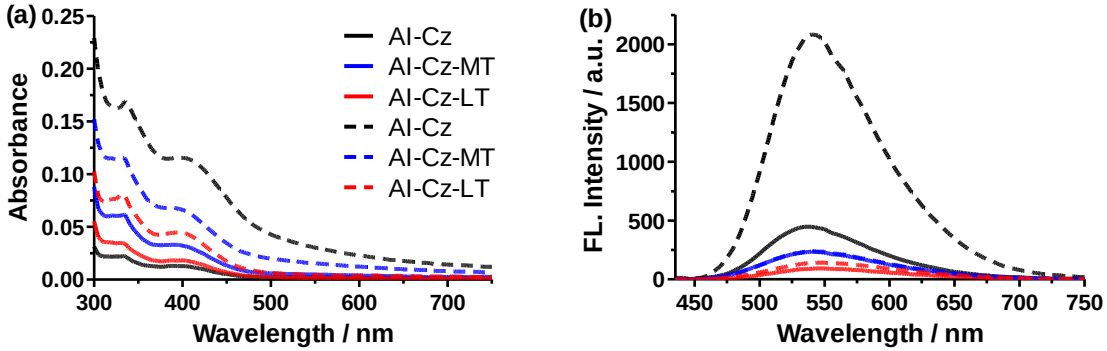

Fig. S2 (a) Absorption and (b) fluorescence emission spectra of 10 μM **AI-Cz**, **AI-Cz-MT** and **AI-Cz-LT** in different solutions. Solid line: 20 mM PBS buffer (pH 7.4) with 2.0% DMSO as co-solvent; dot line: 20 mM PBS buffer (pH 7.4) with the addition of BSA (10 mg/mL). The excitation wavelength is 390 nm.

6. DFT calculations

To ancillary support TADF properties of our probes, the molecular-simulations of **AI-Cz-MT** and **AI-Cz-LT** were performed by time-dependent DFT (TD-DFT) at the B3LYP/ TZP (basis set) with the Amsterdam Density Functional (ADF) 2018 program. We found that the LUMO of **AI-Cz-MT** was mainly localized on the triphenylphosphonium moiety and the HOMO of **AI-Cz-LT** was mainly localized on 2-morpho-linoethylamine moiety owing to interference from the electron density of the organelle targeting moieties. Note that the HOMO→LUMO transition of **AI-Cz-LT** was forbidden, while the HOMO-1→LUMO and HOMO-2→LUMO transitions with approximate energies were allowed (Table S1), which implied that HOMO-1, HOMO-2 and LUMO orbitals can be involved in the TADF process of **AI-Cz-LT**. The LUMO orbital of **AI-Cz-LT** was localized mainly on aromatic imide moiety, whereas the HOMO-1 and HOMO-2 orbitals were mainly distributed on the carbazole units, leading to good spatial separation between HOMOs and LUMOs (Fig. S3a).

Furthermore, DFT calculation of a derivative **AI-Cz-HS** which was removed triphenylphosphonium moiety from **AI-Cz-MT** was performed. As shown in Fig. S3b, the calculated data show that **AI-Cz-HS** have the HOMO/LUMO energy levels are −6.41/−3.36 eV, and the band gap was determined to be 3.05 eV. The HOMO of **AI-Cz-HS** was found to be mainly localized on the carbazole moiety, whereas the LUMO was located on the aromatic imide moiety. All these results could indirectly support TADF properties of **AI-Cz-MT** and **AI-Cz-LT**.

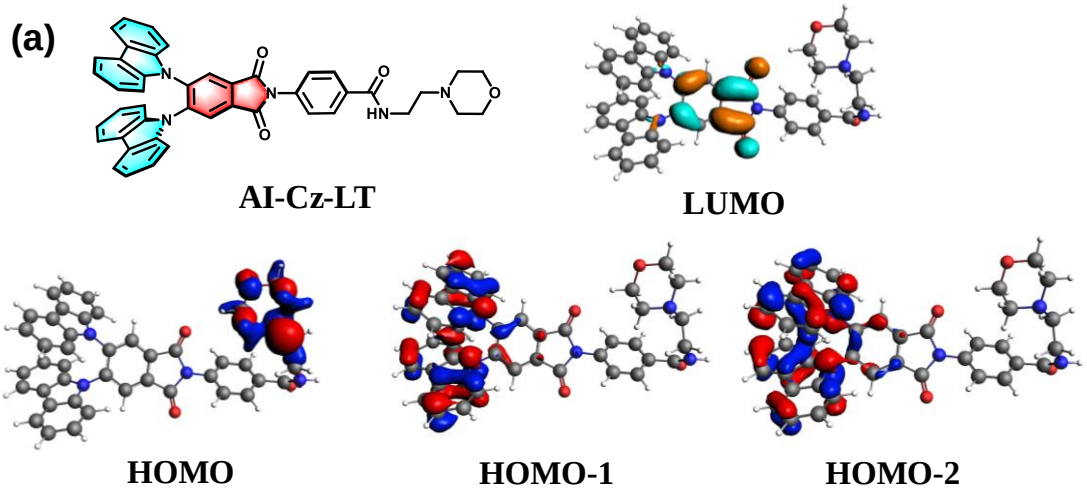

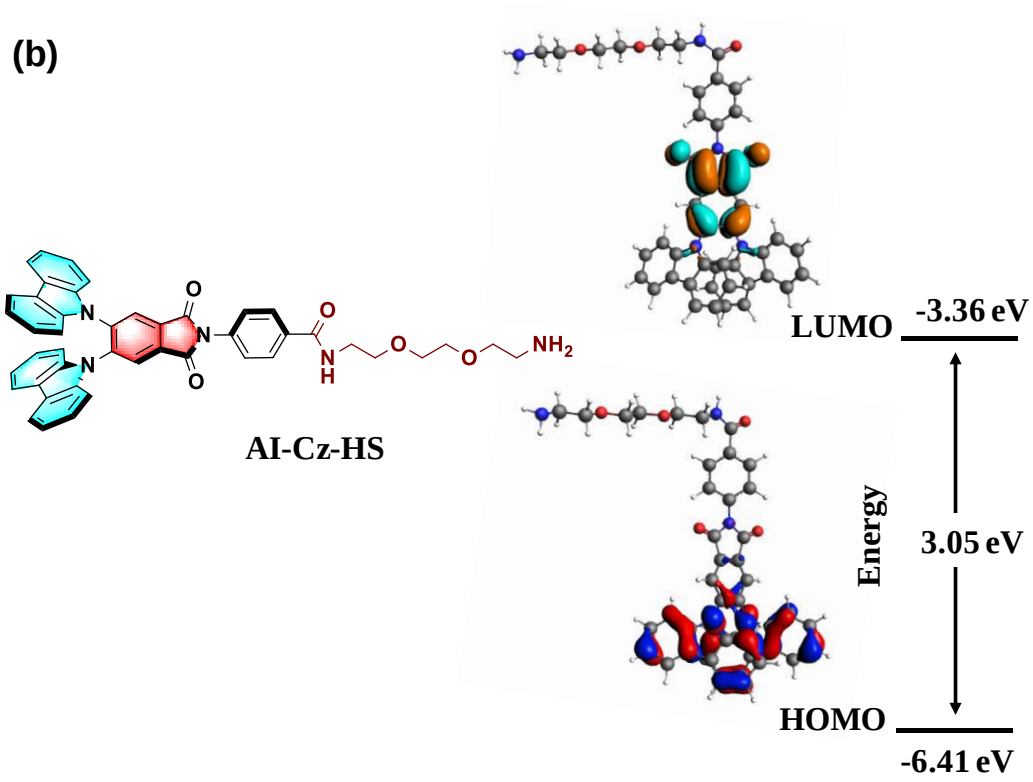

Fig. S3 (a) The HOMO and LUMO distributions calculated by TD-DFT, (a) **AI-Cz-LT**; (b) **AI-Cz-HS**.

Table S1. Computed transition energies (E_{VA}), oscillator strengths (f_{VA}) of AI-Cz-LT and AI-Cz-MT on S_0 geometries optimized by TD-DFT at the B3LYP/ TZP (basis set) with ADF 2018 program.

		S_0 geometry		
		E_{VA} (eV)	**CI description**	**f_{VA}**
AI-Cz-LT	S_1	2.22	HOMO→LUMO	0.000
	S_2	2.50	HOMO-1→LUMO	0.032
	S_3	2.73	HOMO-2→LUMO	0.131

7. TADF characterized data of AI-Cz-MT and AI-Cz-LT

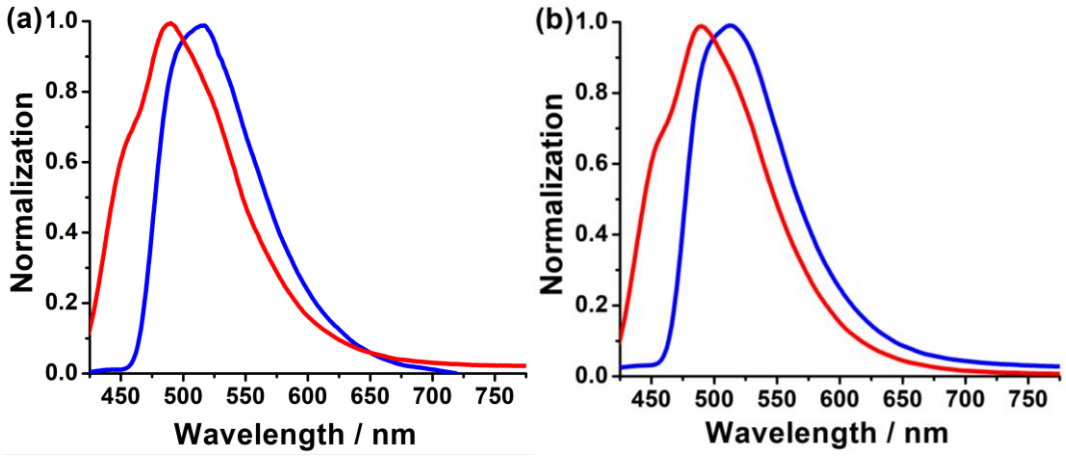

Fig. S4 Fluorescence (red) and phosphorescence (blue) spectra of **AI-Cz-MT** (a) and **AI-Cz-LT** (b) in oxygen-free 2-MeTHF solution at 77 K. Excited at 390 nm.

Table S2. The maximum fluorescence and phosphorescence wavelengths, S_1 and T_1 energy levels, ΔE_{ST} of **AI-Cz-MT** and **AI-Cz-LT** in 2-MeTHF at 77 K and Φ_F at rt.

Compound	**Solvent**	λ_{FL}[a] **(nm)**	E_{S1} **(eV)**	λ_{phos}[b] **(nm)**	E_{T1} **(eV)**	ΔE_{ST}[c] **(eV)**	Φ_F[d] **%**
AI-Cz-MT	2-MeTHF	490	2.53	515	2.41	0.12	7.3
AI-Cz-LT	2-MeTHF	490	2.53	512	2.42	0.11	8.3

[a] Fluorescence emission peaks (c = 10 μM). [b] Phosphorescence emission peaks (c = 10 μM). [c] $\Delta E_{ST} = E_{S1} - E_{T1}$. [d] Absolute fluorescence quantum yield in 2-MeTHF.

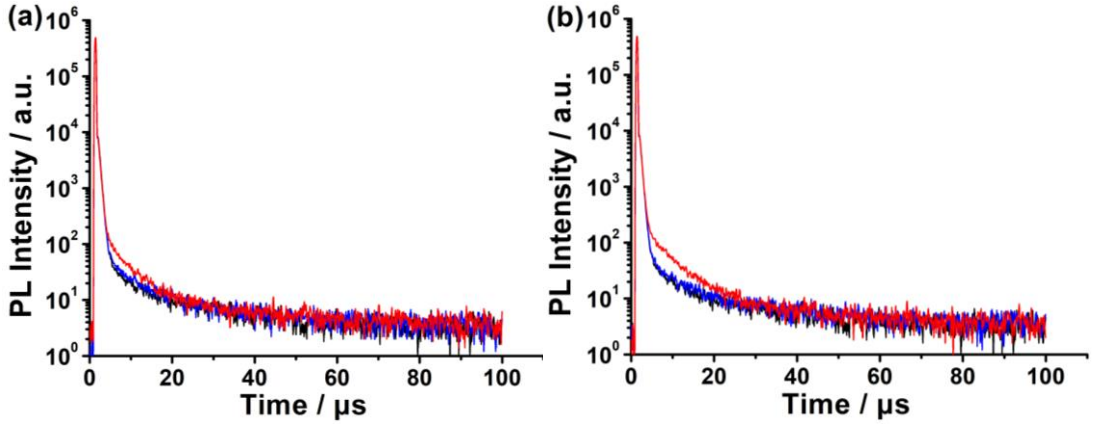

Fig. S5 Fluorescence emission decays of **AI-Cz-MT** (10 μM) and (b) **AI-Cz-LT** (10 μM) in toluene at room temperature, **red** curve shows the profile after deoxygenating and **blue** curve shows the profile under air atmosphere and **black** curve shows instrument response function (IRF). Excited at 375 nm and monitored at 540 nm.

Table S3. Fluorescence lifetime compositions of delayed components of **AI-Cz-MT** and **AI-Cz-LT** (10 μM) in toluene after deoxygenating. Excited at 375 nm and monitored at 540 nm.

Compound	τ_1[a] **(μs)**	n_1[b] **%**	τ_2[a] **(μs)**	n_2[b] **%**	τ[c] **(μs)**
AI-Cz-MT	2.30	19.80	7.16	80.20	6.8

AI-Cz-LT	1.03	8.74	6.40	91.26	6.3

[a] Obtained from the double-exponential fitting of transient decay curves on a 100 μs scale. [b] The contribution of each component to average lifetime. [c] The average fluorescence lifetime of delayed component.

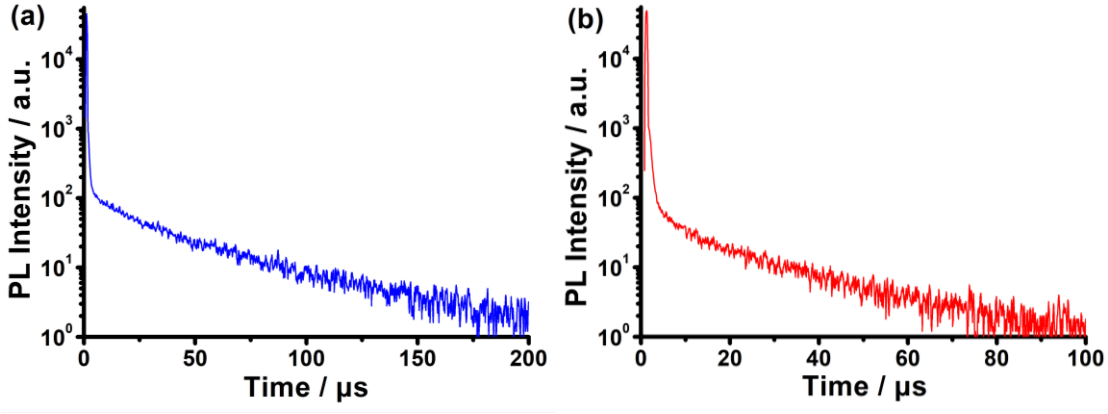

Fig. S6 Fluorescence emission decays of (a) **AI-Cz-MT** (blue curve) and (b) **AI-Cz-LT** (red curve) in solid states without deoxygenating. Excited at 375 nm and monitored at 570 nm.

Table S4. Fluorescence lifetime compositions of delayed components of AI-Cz-MT and AI-Cz-LT in solid states without deoxygenating. Excited at 375 nm and monitored at 570 nm.

	τ_1[a] (μs)	n_1[b] %	τ_2[a] (μs)	n_2[b] %	τ[c] (μs)
AI-Cz-MT	11.15	10.37	44.02	89.63	43.1
AI-Cz-LT	3.59	13.83	21.76	86.17	21.3

[a] Obtained from the double-exponential fitting of transient decay curves. [b] The contribution of each component to average lifetime. [c] The average fluorescence lifetime of delayed component.

Table S5. Fluorescence lifetime compositions of delayed components of **AI-Cz-MT** (10 μM) in PBS solution with the addition of BSA after deoxygenating and without deoxygenating. Excited at 375 nm and monitored at 540 nm.

	τ_1[a] (μs)	**n_1[b] %**	**τ_2[a] (μs)**	**n_2[b] %**	**τ[c] (μs)**
Oxygen-free[d]	0.61	1.13	13.35	98.87	13.3
Atmospheric[e]	2.70	17.61	13.07	82.39	12.6

[a] Obtained from the double-exponential fitting of transient decay curves on a 100 μs scale. [b] The contribution of each component to average lifetime. [c] The average fluorescence lifetime of delayed component. [d] in PBS solution with the addition of BSA after deoxygenating. [e] in PBS solution with the addition of BSA without deoxygenating.

8. HepG 2 cell line and culture conditions

The human hepatoma cell line (HepG 2) used in our experiments was purchased from Cell Resource Centre, Institute of Basic Medical Sciences, Chinese Academy of Medical Sciences & Peking Union Medical College. HepG 2 cells were cultured in DMEM (Dulbecco's modified Eagle's medium) (Corning) containing 10% fetal bovine serum (Invitrogen) and 1% penicillin−streptomycin (Corning). All cell lines were maintained at a humidified incubator with 5% CO_2 at 37 ºC.

9. MTS assay for the cell cytotoxicity

The cytotoxicity of **AI-Cz**, **AI-Cz-MT** and **AI-Cz-LT** was determined by MTS assay *in vitro*. HepG 2 cells were seeded in 96-well flat bottom microtiter plates at a density of 1×10^4 cells/mL with 100 μL per well, incubated in a humidified 5% CO_2 atmosphere at 37 °C for 24 h, then exposed to different concentrations (0-50 μM) of **AI-Cz**, **AI-Cz-MT** or **AI-Cz-LT** for 24 h, respectively. After treatment, 20 μL MTS solution was added to each well and continued to incubate for 3 h. After 3 h incubation at 37 °C, the absorbance was measured at 490 nm with a Tecan Spark™ 10M Multimode Microplate Reader. Cell viability was calculated according to the following formula: Cell viability (%) = $(A\text{-}A_0)$ /$(A_s\text{-}A_0)$ ×100, where A is the absorbance of the experimental group, A_s is the absorbance of the control group, and A_0 is the absorbance of the blank group (no cells). The experiment was repeated three times.

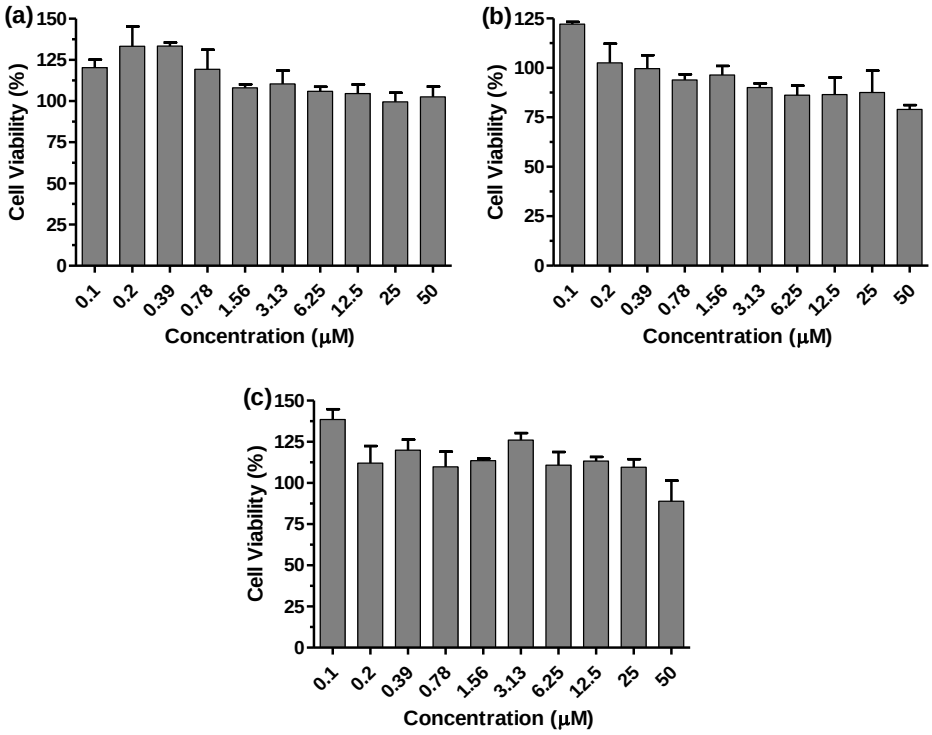

Fig. S7 Cytotoxicity of different concentrations of (a) **AI-Cz**, (b) **AI-Cz-MT** and (c) **AI-Cz-LT** to HepG 2 cells by a standard MTS assay. The experiment was repeated three times and the data are shown as mean ± SD.

10. Confocal imaging of HepG 2 cells treated with AI-Cz, AI-Cz-MT and AI-Cz-LT

Upon reaching 80 % confluence, HepG 2 cells (300 μL, 4×10^4 cells/mL) were transferred into an 8-well chamber containing sterile coverslips at the bottom. On the following day, the media were removed and the cells were washed twice with PBS buffer, then incubated with **AI-Cz**, **AI-Cz-MT** or **AI-Cz-LT** (10 μM) in DMEM medium, respectively. After incubation at 37 °C for 2 h, the cells were washed three times with PBS buffer and were observed with Leica TCS SP8 X Confocal Microscope using 63× magnification. All the probes were excited at 405 nm and the fluorescence was monitored at 450−700 nm.

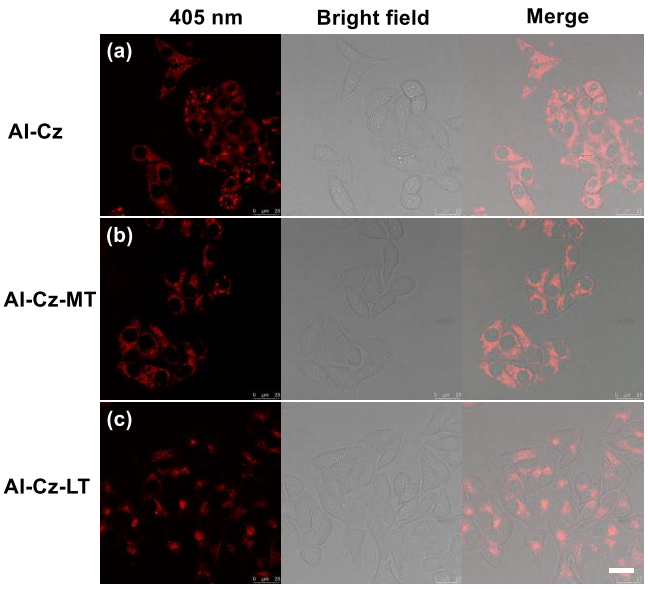

Fig. S8 Fluorescence images of HepG 2 cells staining with 10 μM (a) **AI-Cz**, (b) **AI-Cz-MT** and (c) **AI-Cz-LT**. Probe signal (red): λ_{ex} = 405 nm and λ_{em} = 450-700 nm. Scale bar = 25 μm.

11. Colocalization experiments in HepG 2 cells

Colocalization experiments were conducted by co-staining the HepG 2 cells with appropriate combinations of **AI-Cz-MT** and **AI-Cz-LT** (10 μM) for 2 h and the corresponding commercial organelle markers (200 nM Mito Tracker Green for Mitochondria and 500 nM Lyso Tracker Red DND-99 for Lysosome) for 30 min. Mito and Lyso Tracker were dissolved in DMSO with a concentration of 20 μM and 50 μM respectively to make stock solution for use in fluorescence imaging experiments. Fluorescence imaging experiments were implemented by Leica TCS SP8 X Confocal Microscope using 63× magnification. **AI-Cz-MT** and **AI-Cz-LT** were excited at 405 nm and the emissions were collected in the range of 450-700 nm (channel 1, Red); while Mito Tracker Green was excited at 488 nm and the fluorescence was monitored at 500-540 nm (channel 2, Green), and Lyso Tracker Red was excited at 543 nm and the fluorescence was monitored at 570-620 nm (channel 2, Green). The corresponding Pearson's coefficients were calculated by using the software Image J.

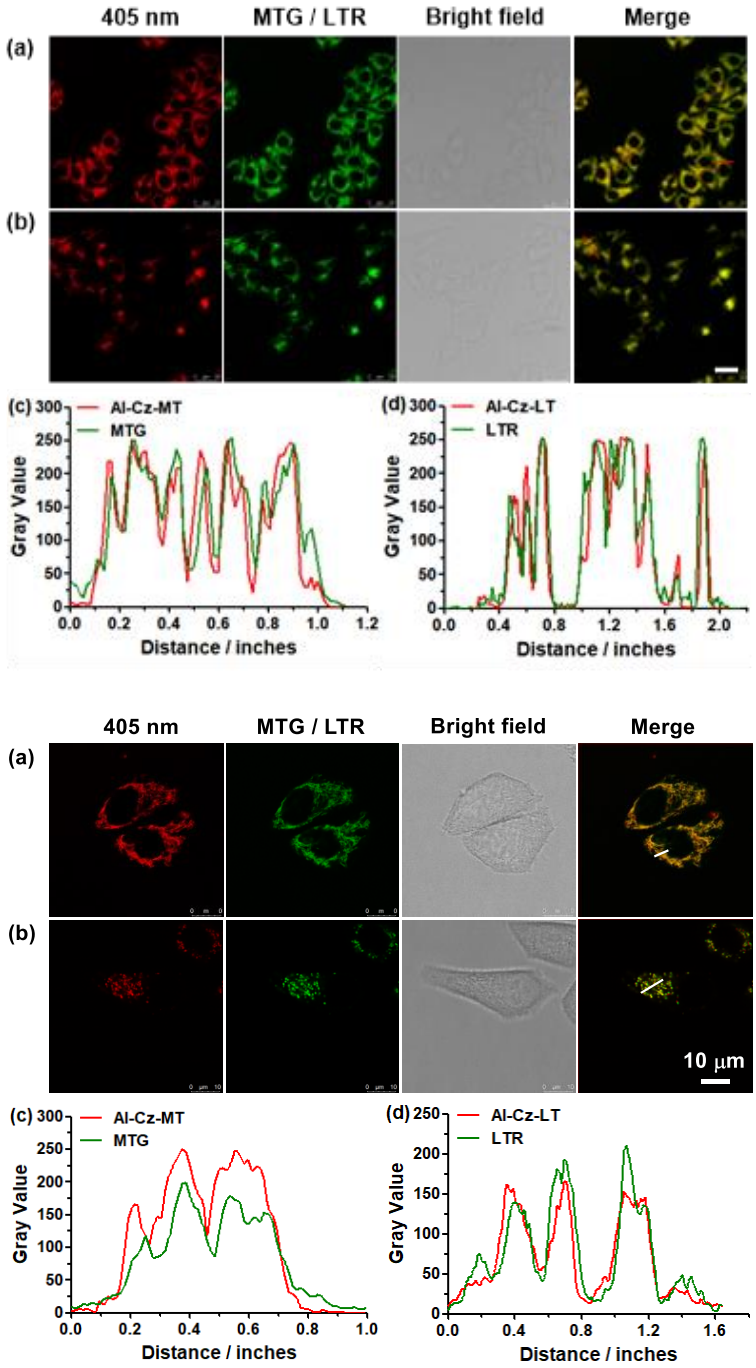

Fig. S9 Subcellular localization of (a) **AI-Cz-MT** and (b) **AI-Cz-LT** in HepG 2 cells. (a) The cells were treated with **AI-Cz-MT** (10 μM) for 2 h and then with Mito Tracker Green (MTG, 200 nM) for 30 min. (b) The cells were treated with **AI-Cz-LT** (10 μM) for 2 h and then with Lyso Tracker Red (LTR, 500 nM) for 30 min. Red channel for **AI-Cz-MT** and **AI-Cz-LT**: λ_{ex} = 405 nm, λ_{em} = 450-700 nm; green channel for MTG (λ_{ex} = 488 nm, λ_{em} = 500-540 nm) and LTR (λ_{ex} = 543 nm, λ_{em} = 570-620 nm). Line profile (c) and (d): the intensity profile of the red/white line in the merged image (a) and (b), respectively. Scale bar = 10 μm.

12. FLIM imaging of HepG 2 cells treated with AI-Cz-MT and AI-Cz-LT

HepG 2 cells were precultured in 24-well plates containing cell culture coverslips to achieve 80% confluence. Then the medium was removed and the cells were incubated with **AI-Cz-MT** and **AI-Cz-LT** (10 μM) in fresh DMEM medium

at 37 °C for 2 h, respectively. After labeling, the cells were washed twice with PBS buffer solution and then fixed by 4% paraformaldehyde. Then, the cells were washed three times with PBS buffer and used for fluorescence lifetime imaging. Fluorescence lifetime images were taken by ISS Q2 confocal laser scanning system coupled to a Nikon TE2000 microscope with the 60×/1.2 NA WI objective lens. The excitation wavelength of the two probes is 405 nm (5000 Hz repetition rate), fluorescence emission and lifetime signals were collected through a 480 nm long-pass edge filter.

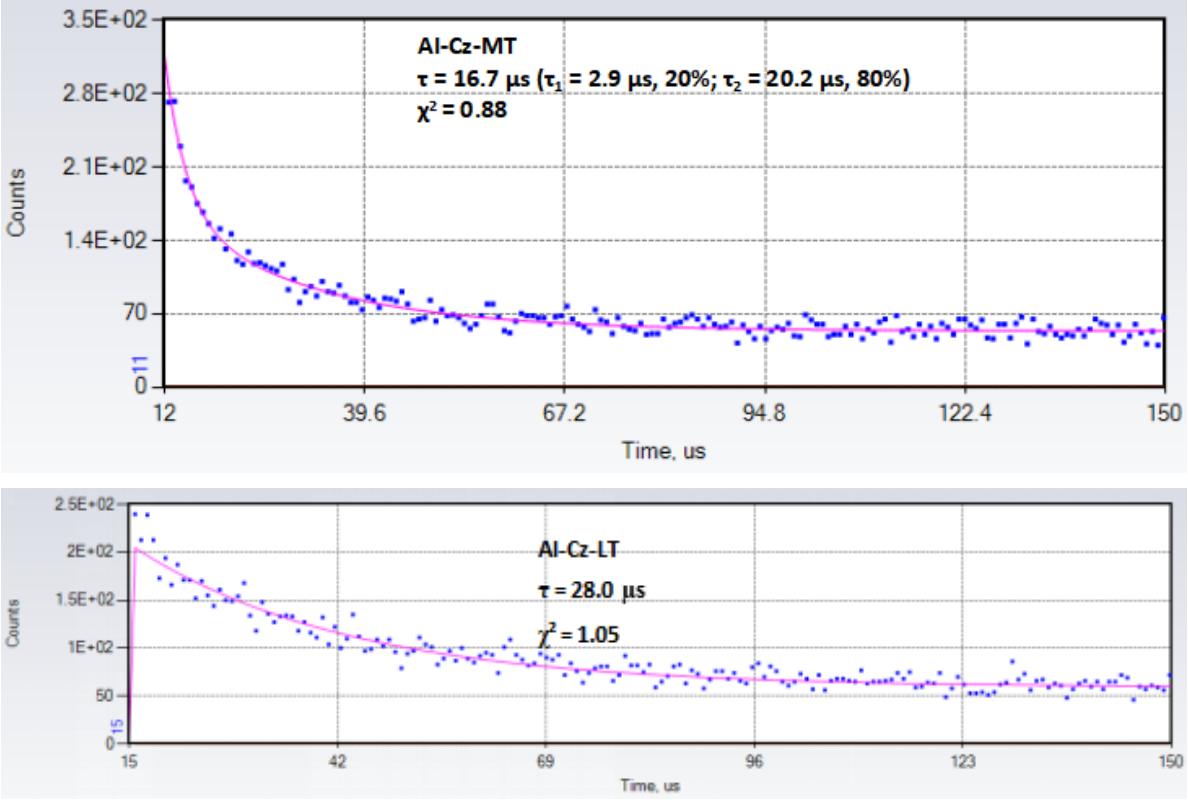

Fig. S10 Corresponding fluorescence lifetime decay curves with reliable two exponentials fitting of **AI-Cz-MT** and one exponential fitting of **AI-Cz-LT** in HepG 2 cells.

13. FLIM imaging of HepG 2 cells treated with AI-Cz-MT and AI-Cz-LT in the addition of BSA

HepG 2 cells were precultured in 24-well plates containing cell culture coverslips to achieve 80% confluence. Then the medium was removed and the cells were washed three times with PBS buffer solution and then fixed by 4% paraformaldehyde for 20 min at room temperature. After fixing, the cells were washed three times with PBS buffer and incubated with **AI-Cz-MT** and **AI-Cz-LT** (10 μM) in PBS solution with the addition of 10 mg/mL BSA for 2 h, respectively. Then, the cells were washed three times with PBS buffer and used for fluorescence lifetime imaging. Fluorescence lifetime images were taken by ISS Q2 confocal laser scanning system coupled to a Nikon TE2000 microscope with the 60×/1.2 NA WI objective lens. The excitation wavelength of the two probes is 405 nm (5000 Hz repetition rate), fluorescence emission and lifetime signals were collected through a 480 nm long-pass edge filter.

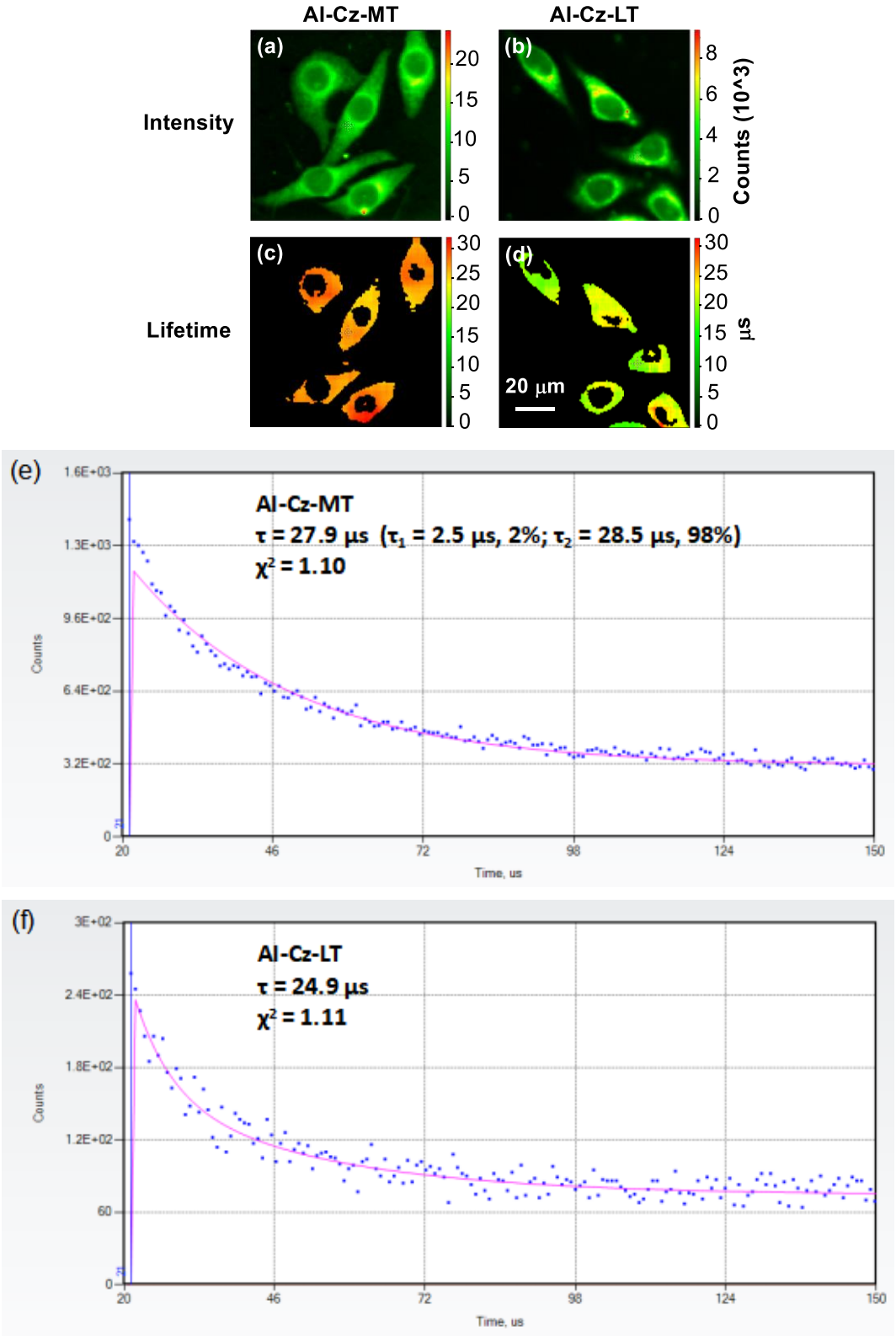

Fig. S11 Fluorescence lifetime imaging of HepG 2 cells stained with (a, c) **AI-Cz-MT** and (b, d) **AI-Cz-LT** (10 μM). Top row: fluorescence intensity; bottom row: lifetime map. The excitation wavelength is 405 nm, and lifetime signals were collected through a 480 nm long-pass edge filter. Scale bar = 20 μm. Corresponding fluorescence lifetime decay curves with reliable two exponentials fitting of **AI-Cz-MT** (e) and one exponential fitting of **AI-Cz-LT** (f) in HepG 2 cells.

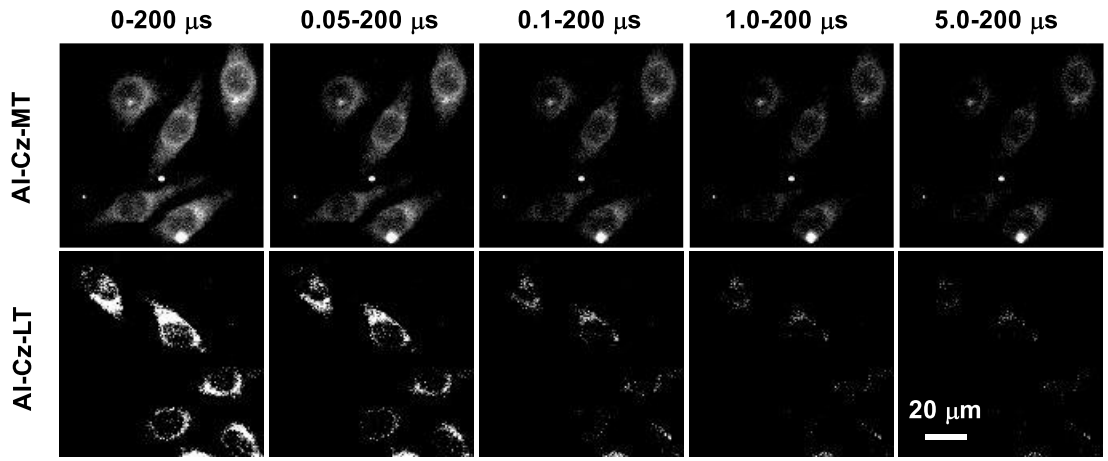

Fig. S12 Time-gated luminescence images of HepG 2 cells stained with AI-Cz-MT and AI-Cz-LT (10 μM) for 2 h in the addition of BSA. Scale bar = 20 μm.

14. Aggregation-induced delayed fluorescence characterized data of AI-Cz-MT and AI-Cz-LT

To clarify the aggregation properties of these two probes, we firstly measured their hydrodynamic radius by DLS in water. The particle sizes of **AI-Cz-MT** and **AI-Cz-LT** were 127.4 nm and 1470.0 nm, respectively (Fig. S13). These results indicated that both probes showed a degree of aggregation in water. However, the solubility of **AI-Cz-LT** in water was very limited and the particle size was large.

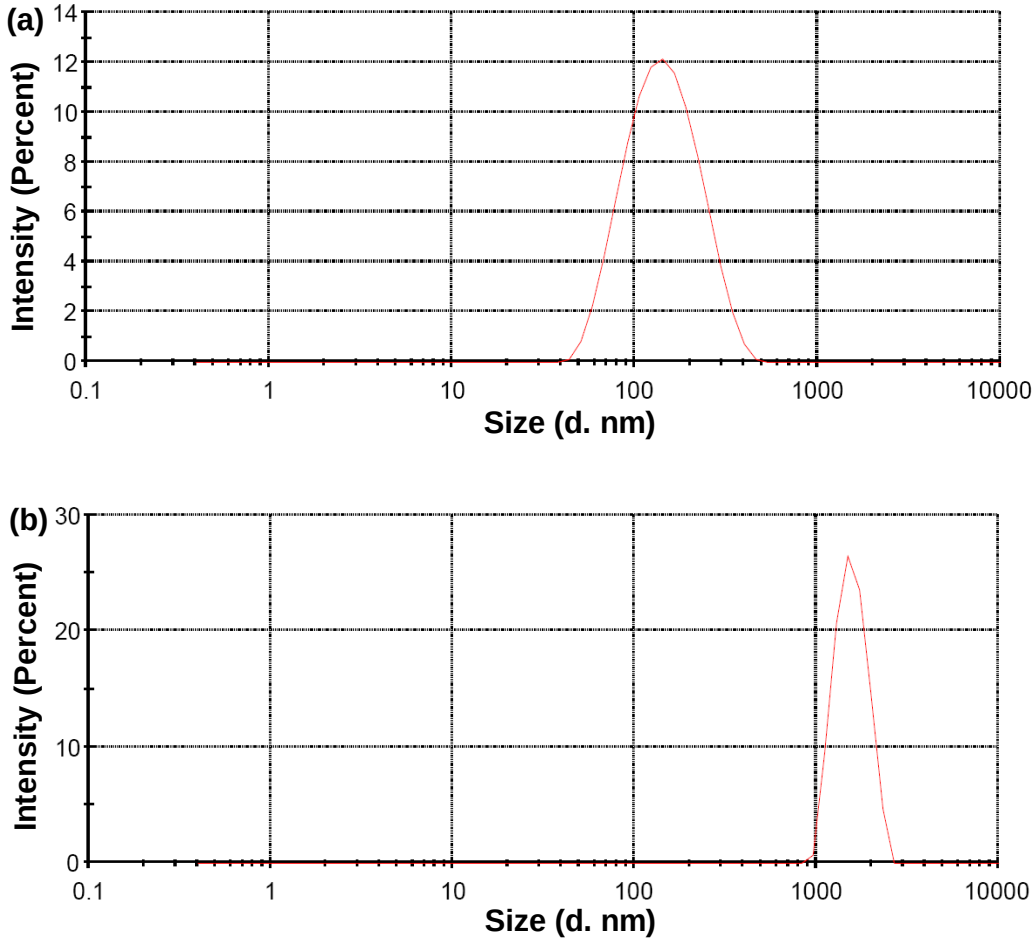

Fig. S13 DLS histograms of **AI-Cz-MT** (a) and **AI-Cz-LT** (b) in water at 50 μM.

Further, we tested the fluorescence lifetime changes of **AI-Cz-MT** and **AI-Cz-LT** in THF/water mixtures with different water fractions (f_w, %) in air condition to clarify if the aggregation could influence the fluorescence lifetime of these two probes or not. With the increase of f_w, the lifetimes of the delayed fluorescence showed no obvious changes, which demonstrated the long lifetimes of **AI-Cz-MT** and **AI-Cz-LT** were not induced by molecule aggregation (Fig. S14). Subsequently, we detected the fluorescence emission decay of **AI-Cz-LT** in PBS buffer (pH 4.0), to mimic the acid environment of lysosome, without deoxygenating, while no delayed fluorescence was observed for probe **AI-Cz-LT** (Fig. S15) either. Therefore, we speculated that the fluorescence emission long lifetime of **AI-Cz-MT** and **AI-Cz-LT** in fluorescence lifetime imaging of HepG 2 cells were not caused by molecule aggregation.

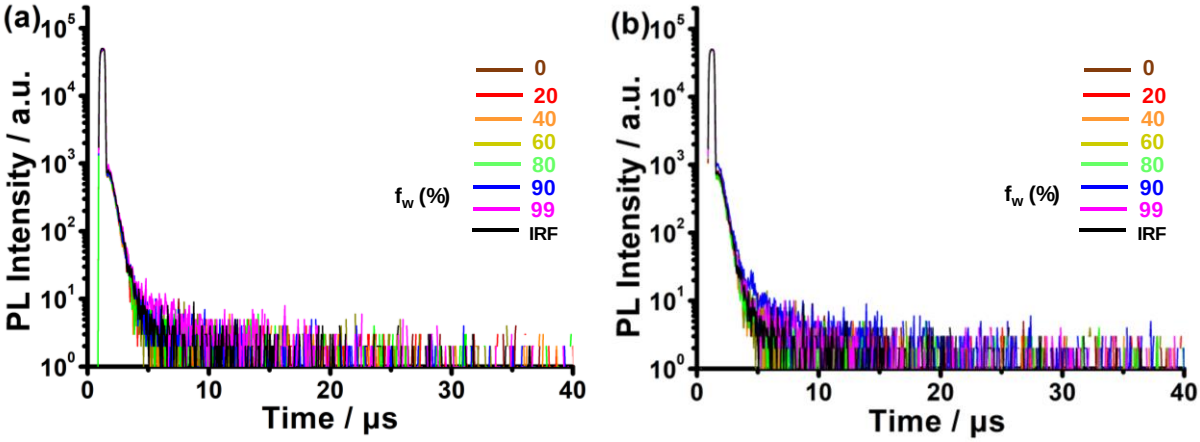

Fig. S14 Fluorescence emission decays of (a) **AI-Cz-MT** (10 μM) and (b) **AI-Cz-LT** (10 μM) in THF/water mixtures with different water fractions (f_w, %) in air condition. Excited at 375 nm and monitored at 570 nm.

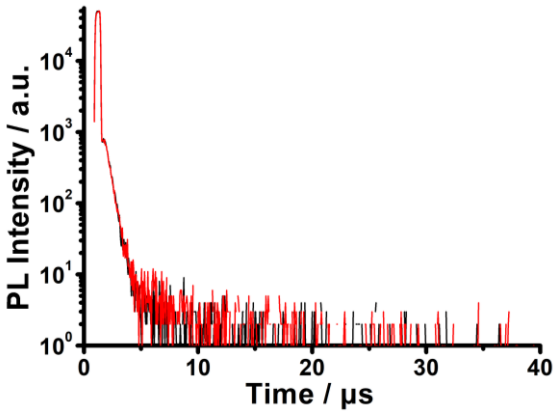

Fig. S15 Fluorescence emission decays of **AI-Cz-LT** (red curve, 10 μM) in PBS buffer (pH 4.0) without deoxygenating and black curve shows instrument response function (IRF). Excited at 375 nm and monitored at 570 nm.

15. Fluorescence characterized data of AI-Cz-MT in various solvents

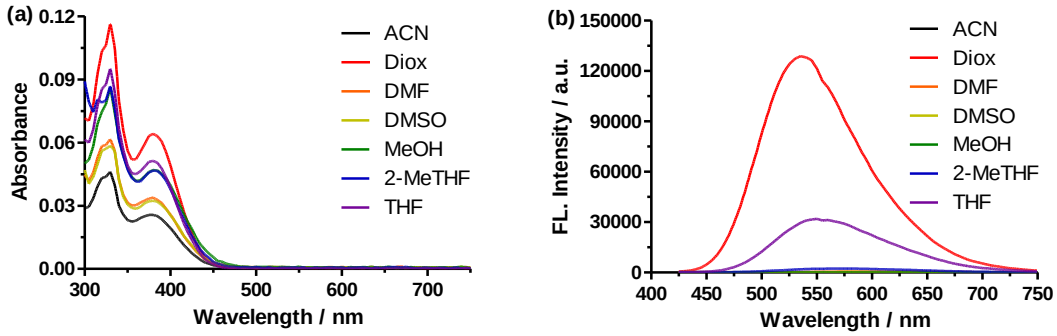

Fig. S16 (a) Absorption and (b) fluorescence emission spectra of 10 μM **AI-Cz-MT** in different polar solvents.

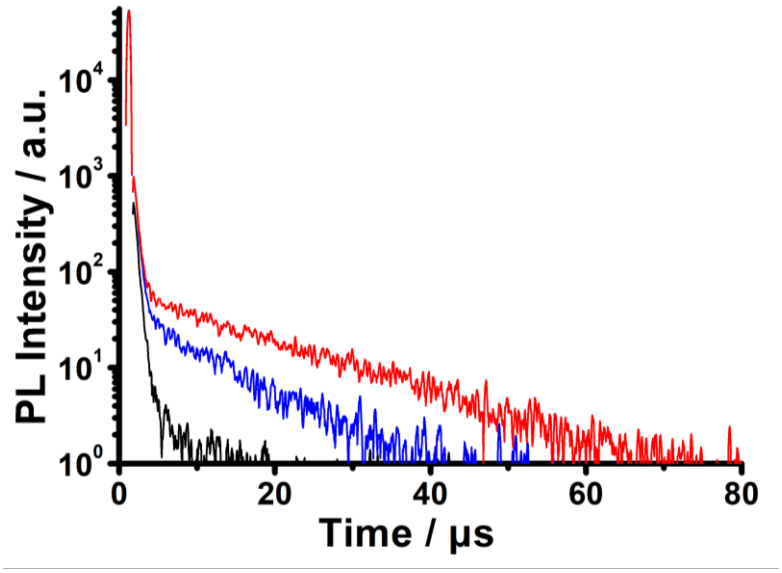

Fig. S17 Fluorescence emission decays of **AI-Cz-MT** (10 μM) in 1,4-dioxane and THF under oxygen-free environment at room temperature, respectively. **Red** curve shows the profile in THF and **blue** curve shows the profile in 1,4-dioxane and **black** curve shows instrument response function (IRF). Excited at 375 nm and monitored at 540 nm in 1,4-dioxane and 550 nm in THF.

Table S6. Fluorescence lifetime compositions of delayed components of **AI-Cz-MT** (10 μM) in 1,4-dioxane and THF after deoxygenating. Excited at 375 nm and monitored at 540 nm in 1,4-dioxane and 550 nm in THF.

Solvent	the Polarity of the solvents	τ_1[a] (μs)	n_1[b] %	τ_2[a] (μs)	n_2[b] %	τ[c] (μs)
1,4-dioxane	4.8	0.45	30.52	8.11	69.48	7.9
THF	4.2	11.42	49.19	26.61	50.81	22.2

[a] Obtained from the double-exponential fitting of transient decay curves. [b] The contribution of each component to average lifetime. [c] The average fluorescence lifetime of delayed component.

16. Copies of NMR spectra of compounds

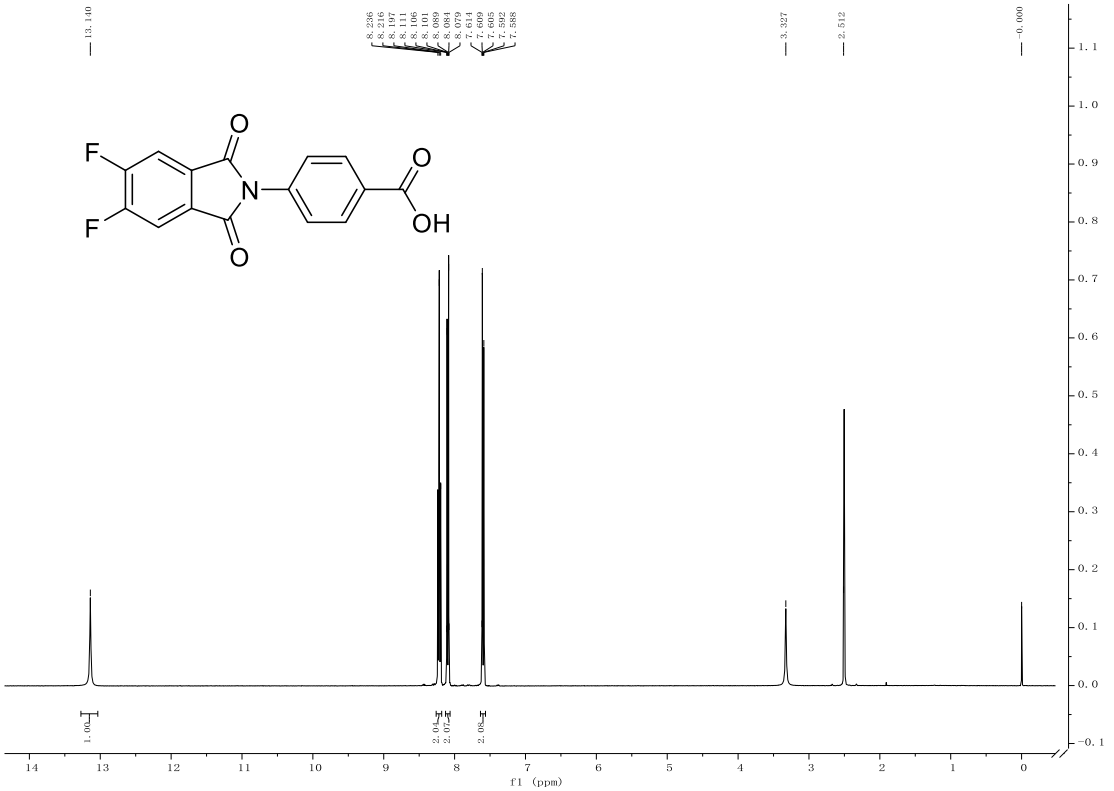

Fig. S18 ^{1}H NMR (400 MHz, DMSO-d_6) of compound **2**.

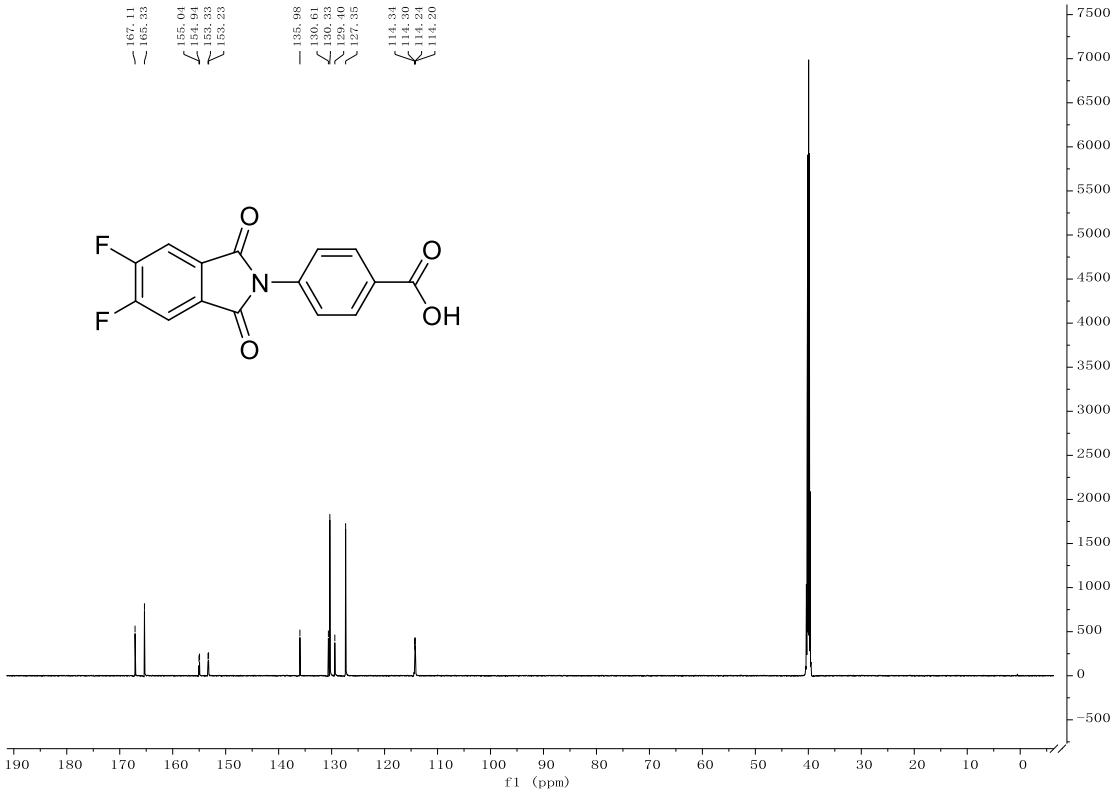

Fig. S19 ^{13}C NMR (150 MHz, DMSO-d_6) of compound **2**.

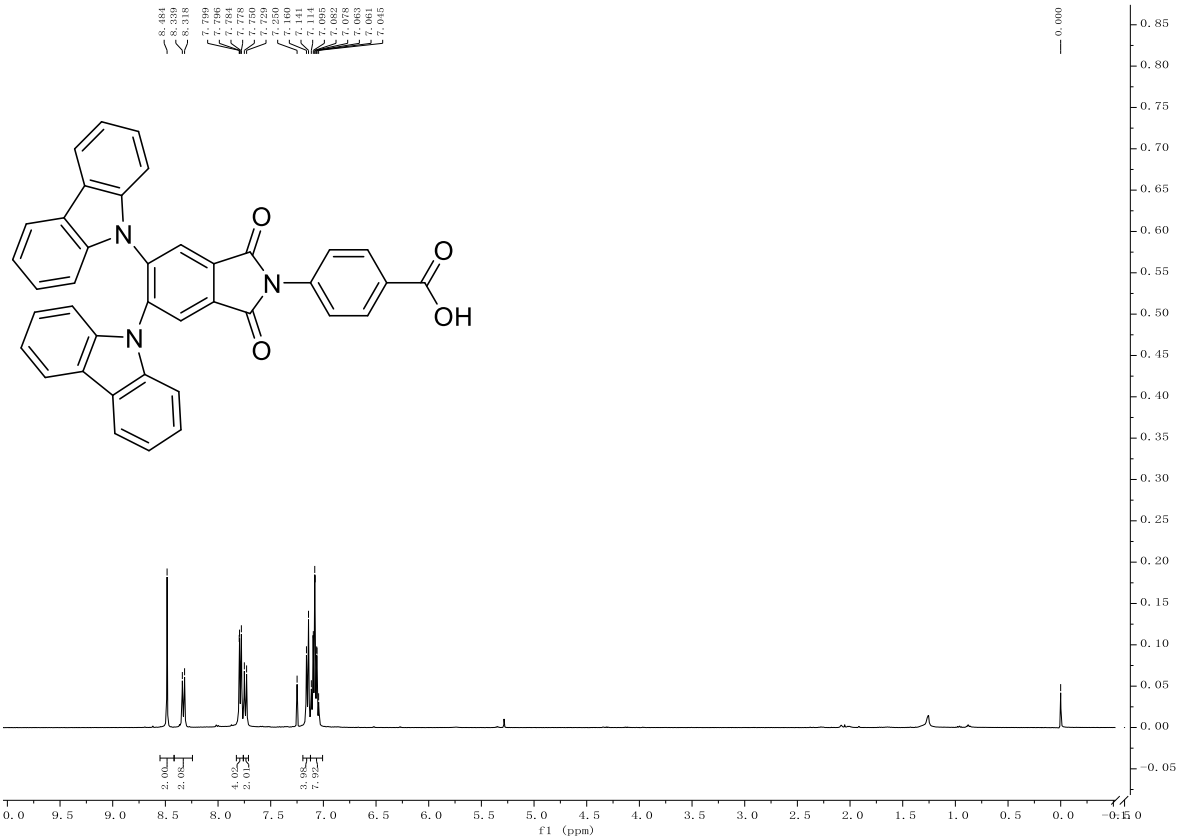

Fig. S20 ^{1}H NMR (400 MHz, $CDCl_3$) of compound **3**.

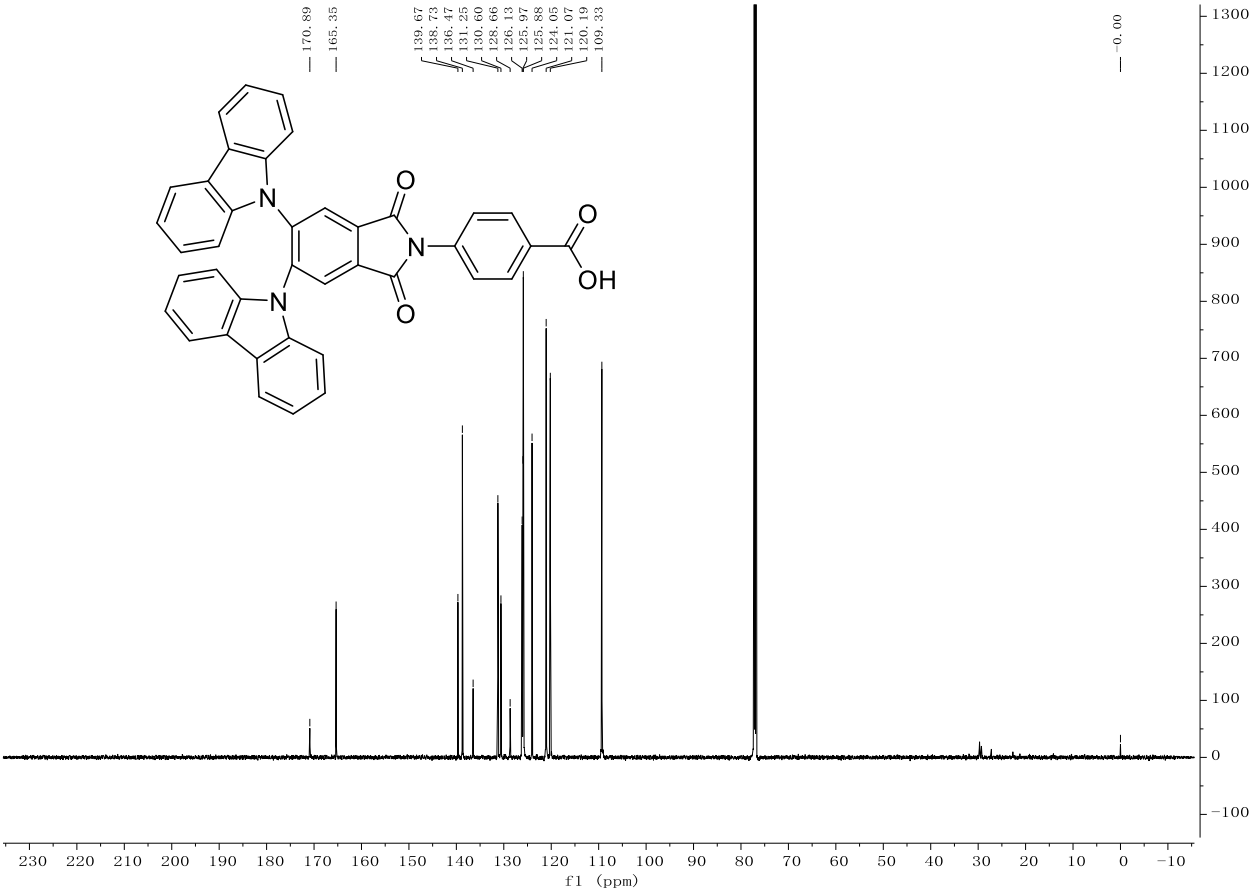

Fig. S21 ^{13}C NMR (150 MHz, $CDCl_3$) of compound **3**.

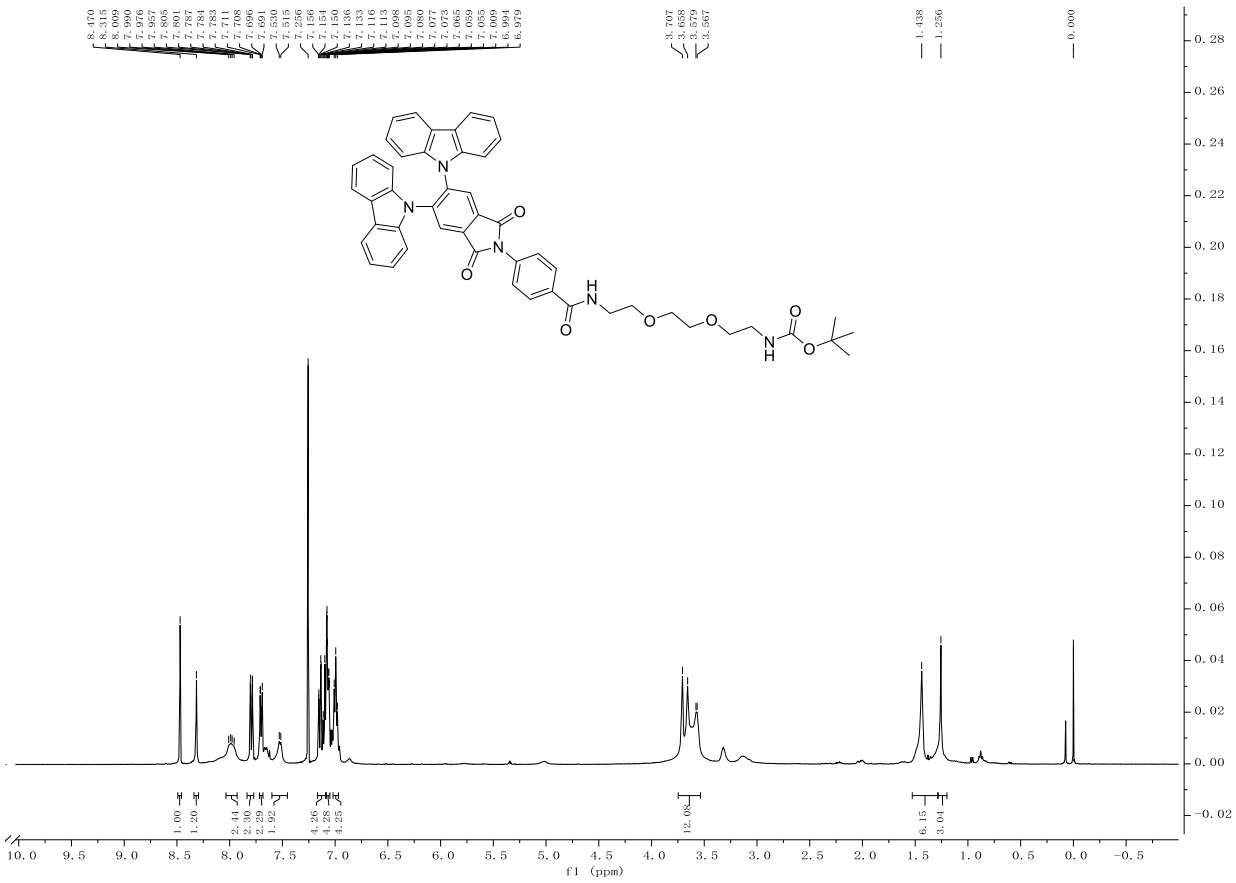

Fig. S22 ^{1}H NMR (400 MHz, $CDCl_3$) of compound **4**.

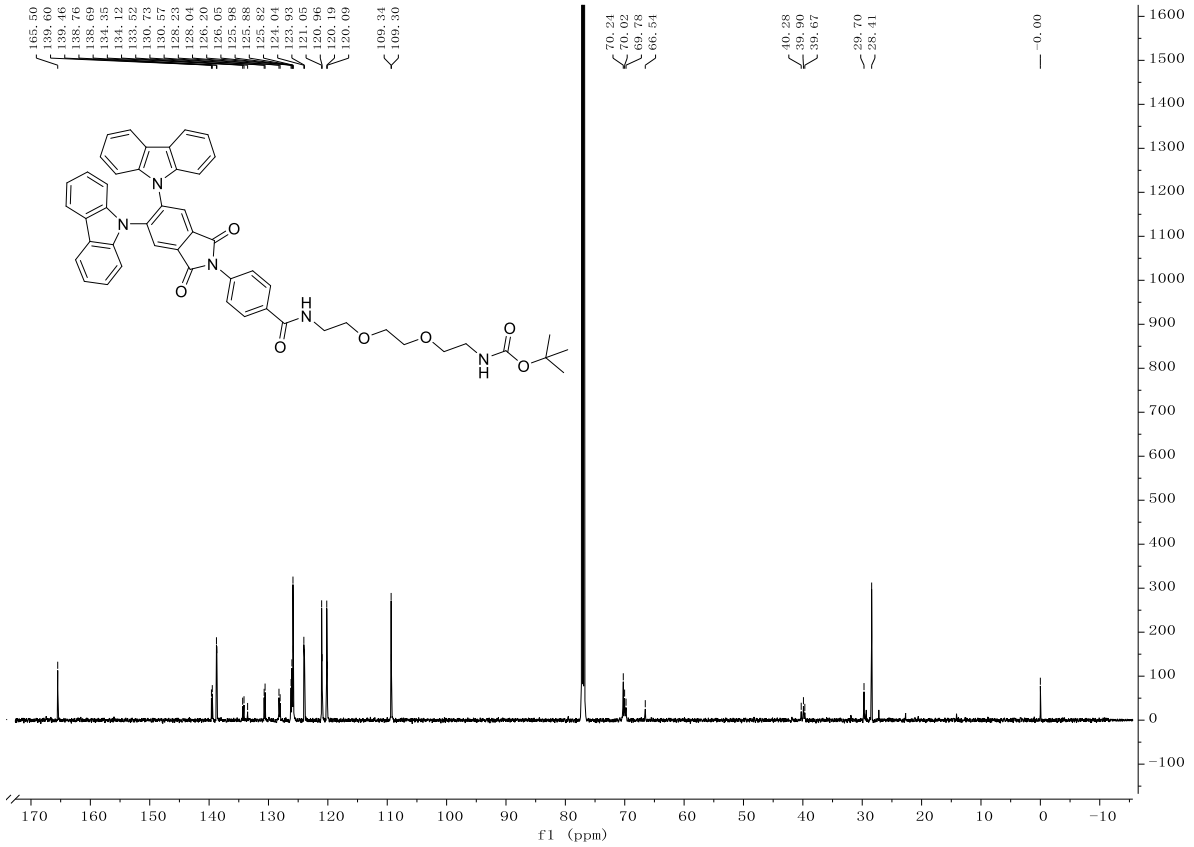

Fig. S23 ^{13}C NMR (150 MHz, $CDCl_3$) of compound **4**.

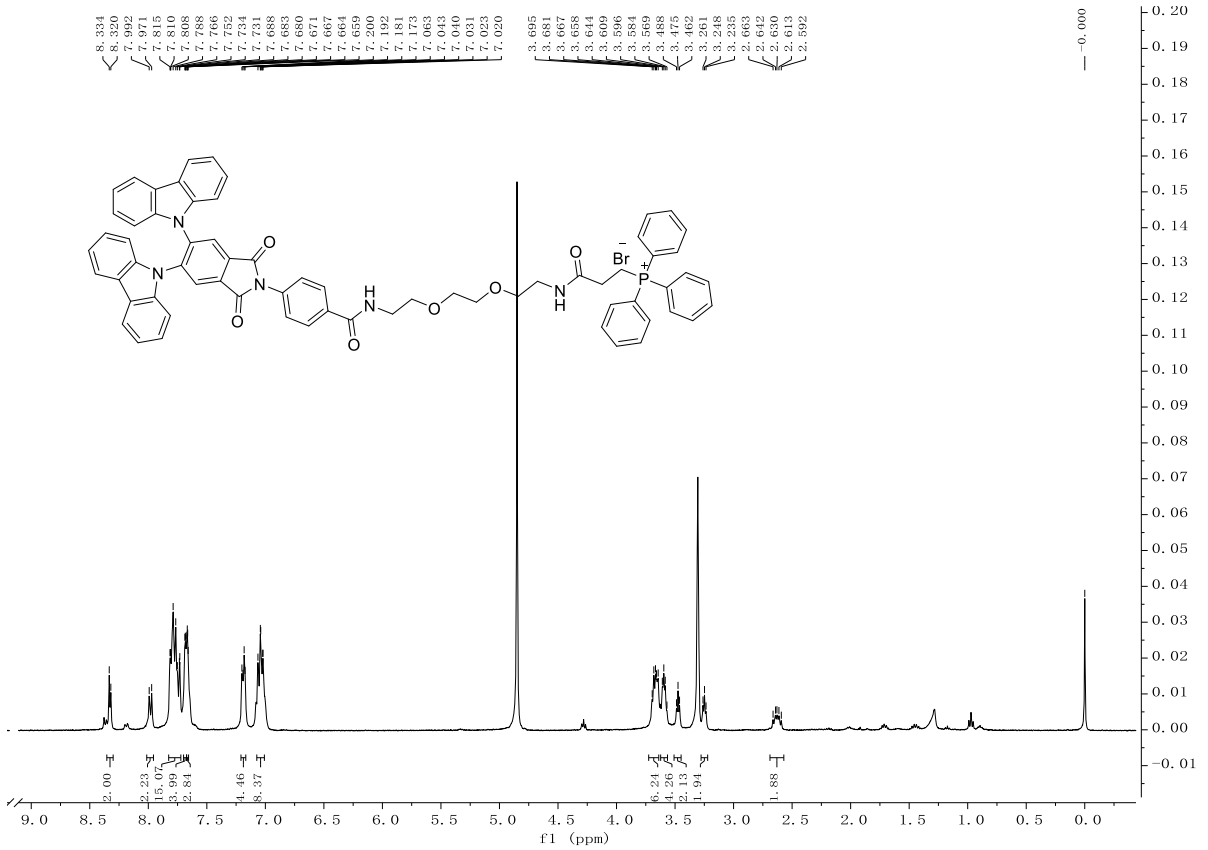

Fig. S24 ^{1}H NMR (400 MHz, Methanol-d_4) of **AI-Cz-MT**.

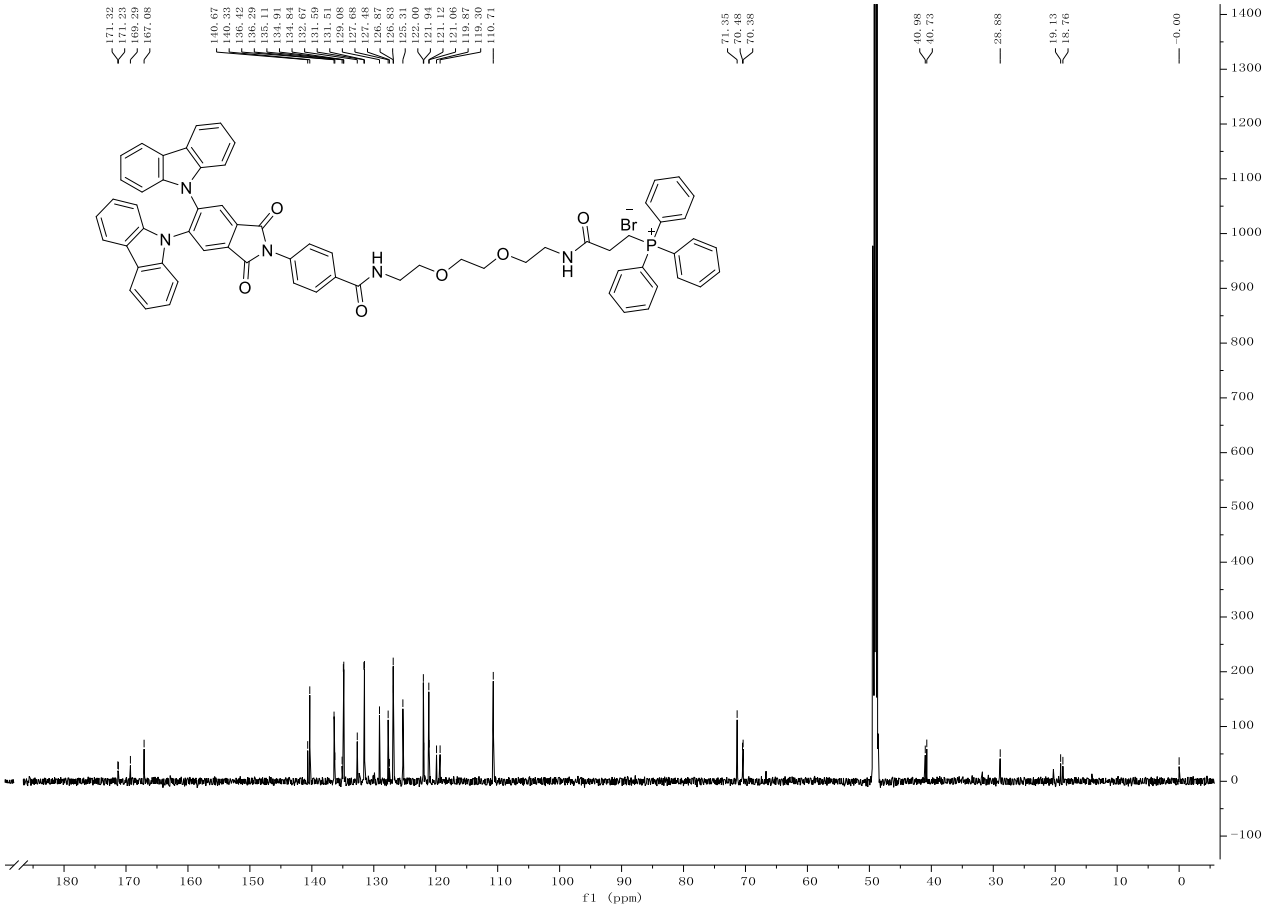

Fig. S25 ^{13}C NMR (150 MHz, Methanol-d_4) of **AI-Cz-MT**.

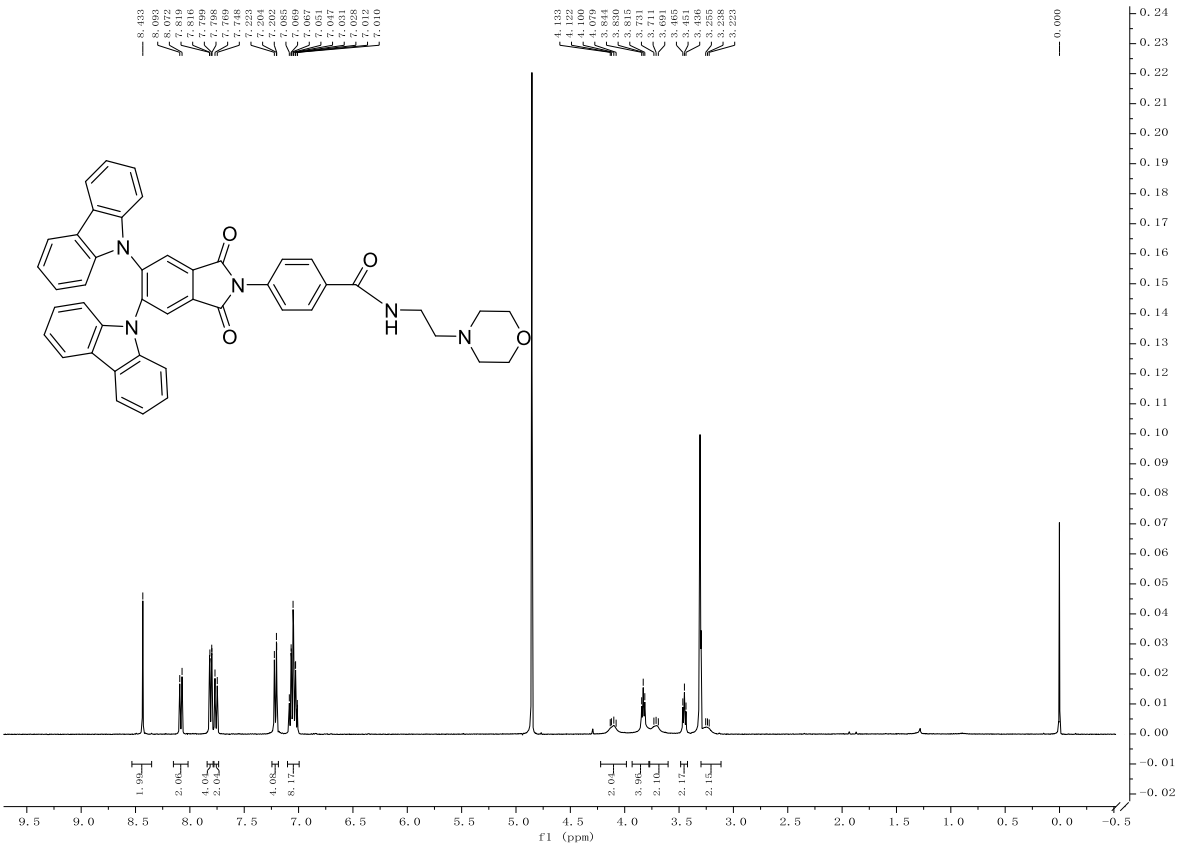

Fig. S26 ^{1}H NMR (400 MHz, Methanol-d_4) of **AI-Cz-LT**.

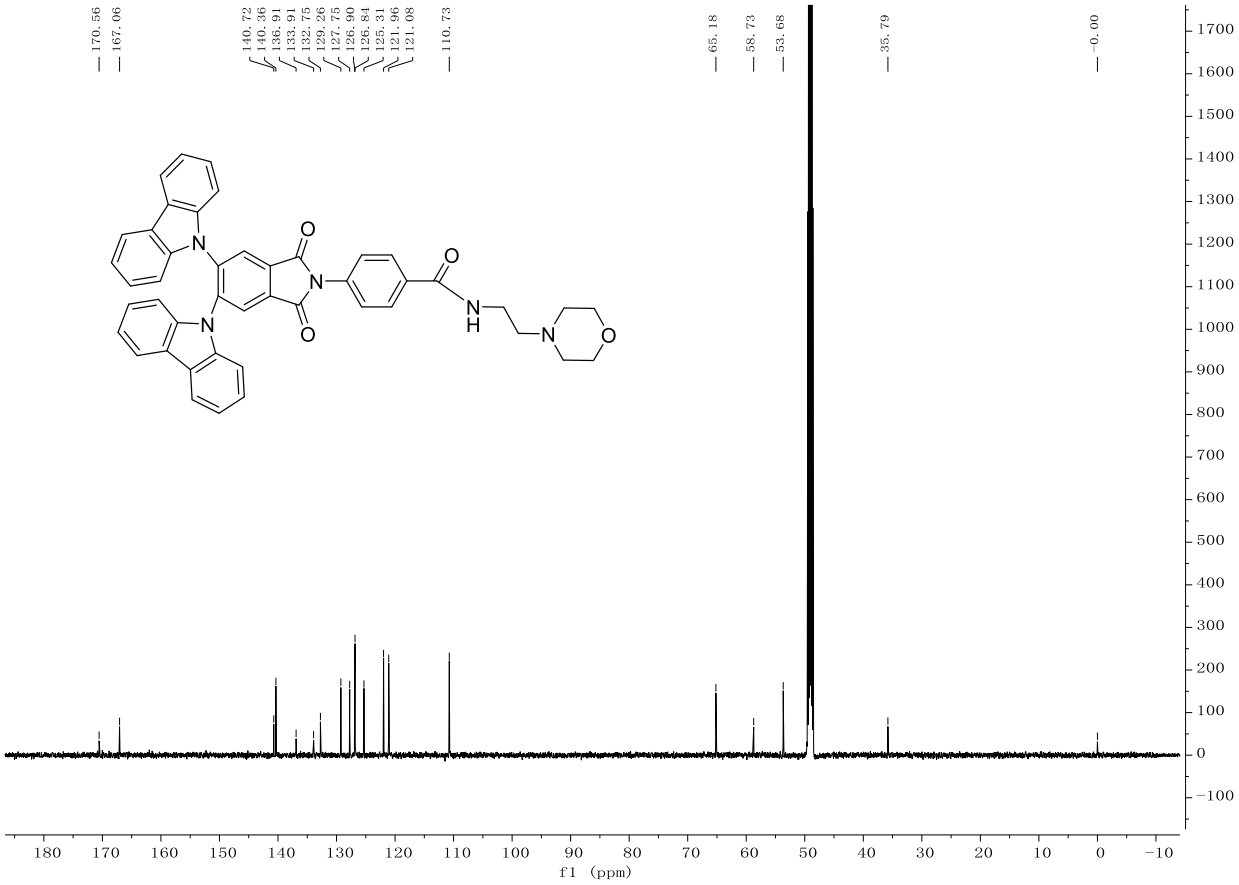

Fig. S27 ^{13}C NMR (150 MHz, Methanol-d_4) of **AI-Cz-LT**.